energies

MDPI

Article

# Investigating the Participation of Embedded VSC-HVDC Systems in Frequency Regulation During Post-Splitting Events via a Coordinated Supplementary Control Layer

**Mohammad Qawaqneh [1,*], Gaetano Zizzo [1], Antony Vasile [1], Liliana Mineo [1], Angelo L'Abbate [2] and Lorenzo Carmine Vitulano [2]**

[1] Department of Engineering, Università degli Studi di Palermo, 90128 Palermo, Italy; gaetano.zizzo@unipa.it (G.Z.); antony.vasile@unibs.it (A.V.); liliana.mineo@unipa.it (L.M.)
[2] Energy Systems Development Department, Ricerca sul Sistema Energetico (RSE), 20134 Milan, Italy; angelo.labbate@rse-web.it (A.L.); lorenzo.vitulano@rse-web.it (L.C.V.)
* Correspondence: mohammad.qawaqneh@unipa.it

**Abstract**

Synchronous Alternating Current (AC) power systems are increasingly supported by embedded High-Voltage Direct Current (HVDC) links to enhance operational flexibility and ensure security of supply. However, the loss of High-Voltage Alternating Current (HVAC) interconnections in these synchronous areas may lead to transmission network splitting, posing serious challenges to frequency stability due to the reduction in overall system inertia and stiffness. In this paper, a supplementary control layer is proposed to enable embedded HVDC systems, particularly those based on modern Voltage Source Converters (VSCs), to support frequency stability under post-splitting conditions. The proposed control strategy combines Angle-Difference Control (ADC), Frequency-Difference Control (FDC), and feedforward action, enabling fast and coordinated active-power modulation. A single-bus, dynamic multi-area Load Frequency Control (LFC) model is developed, combining the regulation of thermal units, Renewable Energy Sources' (RESs') Fast Frequency Response (FFR) with Synthetic Inertia (SI), and VSC-HVDC modulation. The effectiveness of the proposed control layer is demonstrated by applying it to the East Tyrrhenian Link (ETL), an embedded VSC-HVDC interconnection connecting Sicily with the mainland of Italy, under a post-splitting low-inertia condition in which Sicily operates as an islanded synchronous system, i.e., after losing synchronism with the mainland of Italy, in a 2030 scenario condition. The simulation results demonstrate that the proposed controller enables embedded VSC-HVDC systems to actively participate in post-splitting frequency containment and damping, as well as coordinated active power reallocation, thereby enhancing overall system stability and resilience.

**Keywords:** frequency regulation; embedded VSC-HVDC; load frequency control; system splitting; supplementary control

Check for updates

Academic Editor: Jesus C. Hernandez

Received: 28 March 2026
Revised: 17 April 2026
Accepted: 20 April 2026
Published: 23 April 2026

**Copyright:** © 2026 by the authors. Licensee MDPI, Basel, Switzerland. This article is an open access article distributed under the terms and conditions of the Creative Commons Attribution (CC BY) license.

## 1. Introduction

The European power system is undergoing a profound transition driven by the European Union's decarbonization targets [1–3], which are accelerating the integration of inverter-based Renewable Energy Sources (RESs). However, this transition leads to a significant reduction in overall system inertia, posing new challenges for frequency stability and requiring new control approaches that can provide fast and effective frequency support [4].

Modern High-Voltage Direct Current (HVDC) systems, particularly those equipped with Voltage Source Converters (VSCs) technology, can provide an effective solution to these challenges due to their fast and independent control of both active and reactive power, while regulating voltage. These capabilities allow increased operational flexibility and support grid stability [5,6].

In the past, HVDC equipment has been deployed due to the features that have made it preferred over conventional HVAC (High-Voltage Alternating Current) assets for long-distance overhead line and undersea cable power transmission and for asynchronous systems interconnection. The technological progress in power electronics over the last twenty years has contributed to making HVDC more widespread, especially due to boosting VSC-HVDC penetration, in Europe and worldwide [5].

According to their connection to the Alternating Current (AC) network, HVDC projects can be classified as embedded HVDC links, HVDC interconnections, and segmented HVDC systems. An embedded HVDC system is a Direct Current (DC) link with at least two ends being physically connected within a single synchronous AC network. With such a configuration, it can provide not only the basic function of bulk power transmission, but also, very importantly, additional control functions within the AC network, such as power flow control, voltage regulation, system stability improvement, and mitigation of system cascading failures [7]. HVDC interconnections are typically used to connect asynchronous or remote areas, while segmented HVDC systems are used to enhance power transfer between segmented parts of the same network. Back-to-back HVDC links may serve either function, as they can be used to couple asynchronous systems or to segment a synchronous grid while maintaining controllable power exchange [8].

The Tyrrhenian Link (TL) in Italy is one of the most recent examples of VSC-HVDC projects and consists of two parts: the West Tyrrhenian Link (WTL) and the East Tyrrhenian Link (ETL), each with a rated power of 1000 MW. The WTL connects Sicily with Sardinia, and these two islands belong to different synchronous areas, so the WTL is classified as a non-embedded HVDC link, while the ETL connects Sicily with Campania, and both regions are part of the same synchronous area (Continental Europe); therefore, the ETL is classified as an embedded HVDC link [9]. Figure 1 shows the TL project.

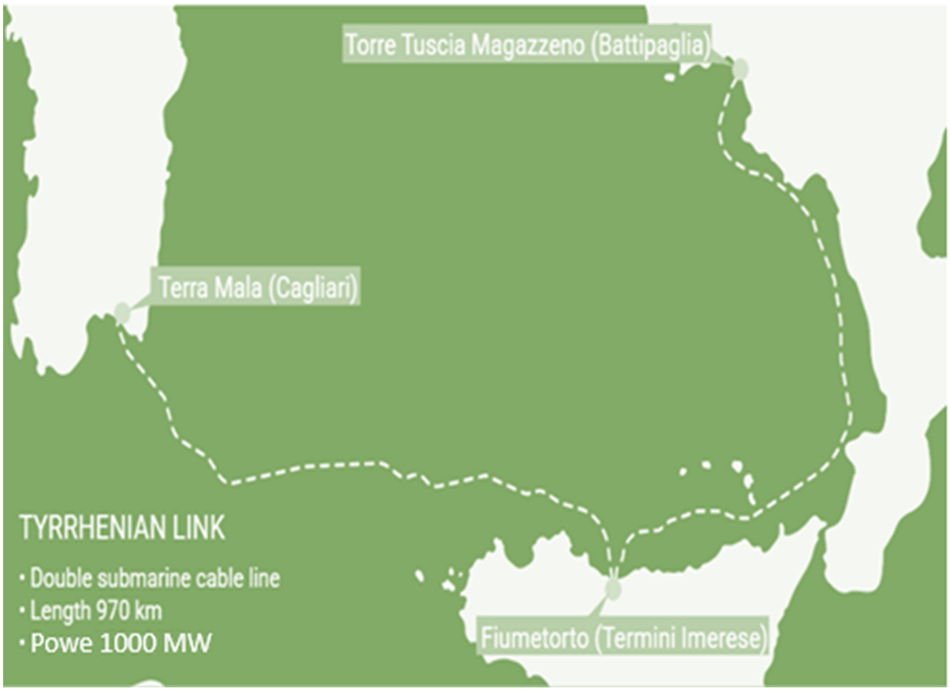


**Figure 1.** Tyrrhenian Link (TL) project (source: [9]).

HVDC links that connect asynchronous areas can provide frequency support following disturbances by modulating their active power flow in proportion to the frequency deviation between their terminals, each located in a different synchronous area [10]. In embedded HVDC systems, where both terminals share the same system frequency, this capability is not feasible under normal operating conditions. Accordingly, the European Network of Transmission System Operators for Electricity (ENTSO-E) does not require embedded HVDC links to operate in Frequency-Sensitive Mode (FSM) and Limited Frequency-Sensitive Mode (LFSM) under normal conditions; however, ENTSO-E specifies that, after system-splitting events, these functions become important and can play a key role in providing effective frequency support [11].

Previous studies have demonstrated the effectiveness of frequency-droop control VSC-HVDC interconnections, such as the WTL, in supporting frequency stability in Sicily during islanded operation under a severe over-generation scenario resulting from the loss of the Sicily–Calabria AC link that serves as an HVAC interconnection with the Italian mainland [12,13]. However, the potential contribution of the ETL has not been investigated due to its embedded nature, and the implementation of a conventional droop control is ineffective under normal operating conditions. Moreover, typical control strategies neglect the electrical-angle separation between the connected areas, which may cause uncontrolled power flow and instability after fault clearance. These aspects motivate the need for an elaborate post-splitting control strategy that accounts for the electrical-angle separation while providing fast frequency support.

In this context, this article extends previous works [12,13] by quantifying the post-splitting frequency support capability of an embedded VSC-HVDC system. A coordinated supplementary control scheme is introduced and evaluated within a dynamic Load Frequency Control (LFC) model, specifically designed for the ETL, through a detailed case study. The proposed approach combines Angle-Difference Control (ADC), Frequency-Difference Control (FDC), and feedforward action to enable fast, coordinated active-power modulation and counteract frequency deviations following the loss of synchronism while accounting for the electrical-angle separation that occurs after system splitting.

The rest of this paper is organized as follows: Section 2 reviews the literature. Section 3 describes the system and dynamic modeling. Section 4 presents the supplementary control scheme proposed for ETL. Section 5 details the case studies. Section 6 discusses the results, and Section 7 concludes the paper.

## 2. Literature Review

Sicily is an ideal case study for investigating frequency stability challenges related to high RES integration and system inertia reduction due to its characteristics, as it combines high RES penetration, planned VSC-HVDC projects such as the TL and ELMED with Tunisia, and a strategic location as a hub between Europe and North Africa. The island can play an important role in supporting national and European decarbonization targets due to its abundant wind and solar resources.

Numerous studies have been conducted on the Sicilian power system to analyze its frequency stability under islanded operating conditions. In [14], the frequency stability of the Sicilian grid during islanded operation following the loss of a diesel generation unit has been investigated, highlighting the potential contribution of RES with different levels of participation in frequency regulation through Fast Frequency Response (FFR) with Synthetic Inertia (SI). The study presented in [15] examined the role of coordinated inertial response from wind kinetic energy and electromagnetic energy stored in equipped supercapacitors on the small-signal stability of the Sicilian network using dynamic simulations with and without the inertial response, showing that appropriate control tuning enhances the small-signal stability.

Further investigation was conducted in [16] based on different simulation scenarios of the Sicilian grid derived from the OSMOSE project. The study emphasized that in future low-inertia power systems, different services such as SI from RES, flexible demand response, and reactive power provision from static converters should be considered and coordinated to maintain overall system stability. Additionally, power system stability analysis for Sicily's network was conducted in [17] within the OSMOSE project, under 2050 operating conditions, including islanded operation. The study showed the active participation of both demand-side and renewable resources in maintaining voltage and angle stability, despite the reduction in system inertia and thermal regulation.

In addition, the transmission interconnections with Sicily have been analyzed with respect to system stability and secure operation. In [18], the Malta–Sicily Extra-High-Voltage (EHV) AC interconnection was analyzed with a focus on the maximum transmitted power, load flow analysis, short-circuit level, and small-signal stability without considering RES participation in frequency regulation. The study showed an improvement in overall transmission efficiency due to the implementation of an innovative controller scheme. Also, in [19], both static and dynamic analyses were conducted to evaluate the Tyrrhenian Link's contribution to system stability and security of supply under high-voltage grid contingencies; the results highlighted the important role of this project in improving system flexibility and damping inter-area oscillations under 2030–2040 operating scenarios. In [20], the dynamic behavior of the Sicilian grid, including the TL and the HVDC interconnection with Tunisia (ELMED), was analyzed under high RES penetration and different operating situations, showing the positive impact of incorporating grid-forming HVDC interconnections and advanced frequency support control strategies on the transient response of the Sicilian network.

In [21], the opportunities and challenges of grid-forming VSC-HVDC converters were investigated, with a focus on their capability to provide frequency and voltage support in Mediterranean interconnections, showing that significant benefits can be achieved from VSC-HVDC in enhancing system frequency stability and flexibility. However, the operation of embedded VSC-HVDC links under post-splitting conditions with coordinated angle difference, frequency difference, and feedforward control actions integrated within the LFC framework has not been widely explored.

## 3. System Description and Dynamic Modeling

This section describes the portion of the Continental Europe ENTSO-E system considered in the analysis and the dynamic model used to represent the regulation response of thermal units, RES, and VSC-HVDC interconnections.

### *3.1. Identification of the Portion of the ENTSO-E Model*

The analysis focuses on the portion of the Continental Europe ENTSO-E network in a 2030 scenario that includes Sicily and its current and future (planned and under construction) interconnections with Sardinia, the mainland of Italy, Malta, and Tunisia. These interconnections influence the Sicilian system's behavior during disturbances. Schematically, the portion of the network under study is shown in Figure 2.

### *3.2. Model Development*

This study aims to evaluate Sicily's frequency metrics, regulation margins, and active-power reallocation after system splitting of the Sicilian with respect to the Italian mainland AC network, in a 2030 perspective scenario case. For this purpose, a multi-area Load

Frequency Control (LFC) model is developed to represent Sicily, Sardinia, and mainland Italy. This approach is widely used in previous studies [22–27] and is well-suited for system-level frequency stability analysis, as it captures electromechanical dynamics governing frequency response while neglecting fast electromagnetic and voltage dynamics, as reported in [28].

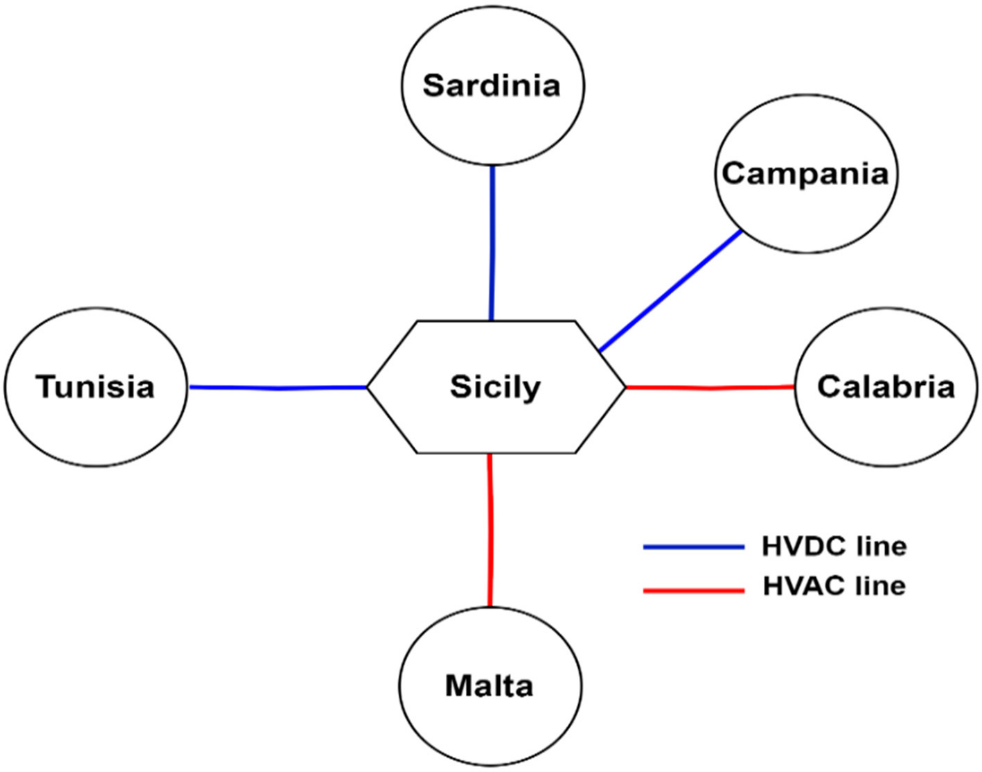


**Figure 2.** Identification of the portion of the network under study.

Each area includes aggregated thermal unit regulation, RES regulation, and VSC-HVDC active-power modulation. The mainland of Italy is modeled as an infinite bus, which is a common assumption in system-level studies of the Sicilian grid [29]. Therefore, the frequency deviation at the ETL mainland terminal is assumed to be zero.

This hypothesis holds because we are focusing on the frequency variations on the two islands, Sicily and Sardinia, and not the impact on the Continental Europe Synchronous Area (CESA), of which Italy is an integral part. In fact, the power–frequency characteristics of the two islands are on the order of hundreds of MW/Hz, while those of the CESA vary, according to the latest estimates, between 19,500 and 27,300 MW/Hz [30,31]. The disturbances considered in this study will therefore cause frequency variations in the synchronous area, and thus in mainland Italy, that will be negligible compared to those in Sicily and Sardinia, which justifies the use of the infinite bus assumption.

The adopted model cannot capture the local phenomena like voltage dips, electromagnetic transients, and the detailed dynamic behavior of PLLs in the VSC-HVDC systems under post-splitting events. These limitations are consistent with the electromechanical scope of this study, which focuses on system-level frequency and active power support.

The objective of this model is to assess the contribution of the embedded ETL in supporting Sicily's frequency stability following a system-splitting disturbance. At the considered operating point conditions, the Sicily–Tunisia (ELMED) and Sicily–Malta interconnections are assumed to operate under fixed-power mode, while the WTL provides frequency droop regulation. The ETL is modeled as an embedded VSC-HVDC link whose active power can be modulated by the proposed supplementary control schemes described in Section 5. Figure 3 illustrates the primary LFC model, which represents Sicily and

Sardinia connected via the WTL, while the ETL is integrated as an additional controllable VSC-HVDC link.

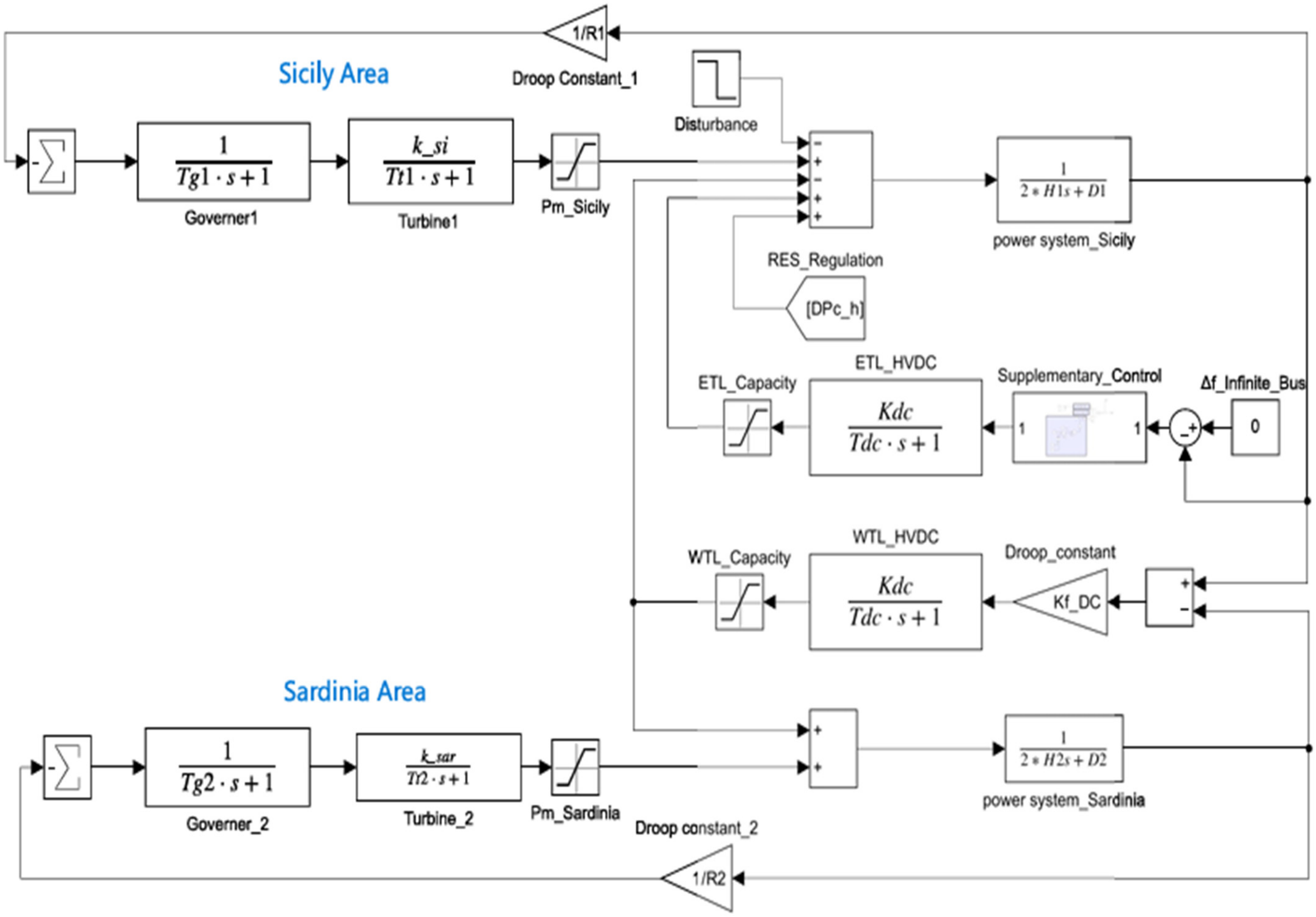


**Figure 3.** Primary LFC model of Sicily–Sardinia system with ETL integration.

Thermal-unit dynamic response is represented by an equivalent governor, turbine, and generator/load chain, which is widely adopted in LFC studies [10,32], as described below:

- Governor model:

$$G_g(s) = \frac{1}{1 + \tau_g s} \tag{1}$$

- Turbine model:

$$G_t(s) = \frac{1}{1 + \tau_t s} \tag{2}$$

- Generator/load model:

$$G_{gl}(s) = \frac{1}{2Hs + D} \tag{3}$$

where $\tau_g$ and $\tau_t$ are the governor and turbine time constants, $D$ represents the load damping factor, and $H$ is the equivalent system inertia constant.

The RES frequency regulation response combines both FFR based on droop control and (SI). Under droop-based regulation, RES converters adjust their active-power output according to the droop characteristic, while energy storage systems are required if the desired power modulation exceeds the RES capability [33].

The RES converters provide SI during the first instants following the disturbance and provide fast active power support. The emulated power *pi*, delivered or absorbed by SI, is defined as follows [34]:

$$\Delta pi = \begin{cases} -K\_\text{in} * f * df/dt,\ df/dt < RoCoF\text{max} \\ -P\text{max} * sign\ df/dt, df/dt \geq RoCoF\text{max} \end{cases} \quad (4)$$

The control gain K_in is selected to enable the SI unit to deliver its maximum capacity when the *RoCoF* reaches a predefined fraction *K*% of its maximum acceptable value. Accordingly, K_in is defined as

$$K\_\text{in} = \frac{P_{max}}{f_0 K\% RoCoF_{max}} \quad (5)$$

where $f_0$ is the nominal frequency, and *K*% represents the fraction of *RoCoF* at which the SI delivers its full capability. To improve the practical implementation of the SI controller, a low-pass filter is applied to the frequency signal to mitigate noise effects on RoCoF estimation [35]. Additionally, a time delay of 50 ms [36] is introduced to represent the measurement delay dynamics. Figure 4 shows the control loop of RES FFR with SI.

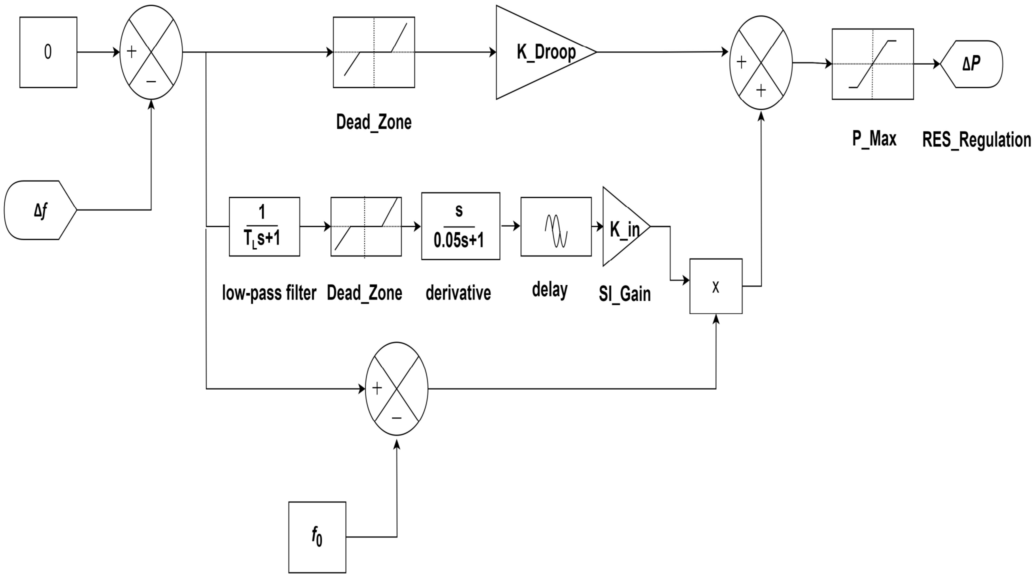


**Figure 4.** RES fast frequency regulation with Synthetic Inertia support.

In [13], the WTL operates under a frequency-droop controller enabling effective and fast active power modulation between Sicily and Sardinia. The power $\Delta P_{DC}$ transferred between Sicily and Sardinia in response to a frequency deviation $\Delta f$, as the following equation shows [37]:

$$\Delta P_{DC} = \mathrm{K}_{\mathrm{f\_DC}}\ \Delta f \quad (6)$$

where $\mathrm{K}_{\mathrm{f\_DC}}$ is the droop coefficient representing power change in response to frequency deviation. In dynamic LFC studies, the VSC-HVDC link is represented by a first-order transfer function [37,38]:

$$G(s) = \frac{Kdc}{(1 + Tdcs)} \quad (7)$$

where *Kdc* is the gain constant of the converter/rectifier unit, and *Tdc* is the time constant of the converter (s). *Kdc* = 1 p.u and *Tdc* = 0.2 s are adopted in this study as used in [13]. A ramp-rate limit of 1000 MW/s is assumed for the HVDC active power modulation, consistent with values reported in [39,40] for modern VSC-HVDC systems. In addition, a limiter is included to reflect the actual capability of the HVDC link.

## 4. Supplementary Control Strategy for the East Tyrrhenian Link

Under normal operating conditions, the ETL operates as an embedded VSC-HVDC interconnection within a single synchronous area. Consequently, it cannot provide frequency support since both terminals of ETL experience the same frequency. However, after a system-splitting event, a frequency deviation appears between its terminals; the ETL can contribute to transient stability by modulating its active power flow. To enable this capability, a supplementary control layer is proposed. The HVDC power flow can be divided into two parts as follows:

$$P_{HVDC} = P_0 + \Delta P_{HVDC} \tag{8}$$

where $P_0$ is the scheduled power set by the operator, and $\Delta P_{HVDC}$ is the modulated power flow introduced by the supplementary control. In dynamic models, this modulation is introduced based on the frequency deviation. To achieve fast and effective controllability of VSC-HVDC, three supplementary control actions are proposed, all based on the following control law [41]:

$$\Delta P_{HVDC} = \underbrace{k_\delta(\delta_1 - \delta_2)}_{ADC} + \underbrace{k_\omega(f_1 - f_2)}_{FDC} + \underbrace{k_{ff}(P_0 - P_{meas})}_{Feedforward} \tag{9}$$

- Angle-Difference Control (ADC)

ADC, also known as AC line emulation, enables VSC-HVDC links to emulate the synchronizing behavior of a conventional AC transmission line [42]. In AC systems, the active power flow between two nodes depends on their voltage-angle difference according to the power angle equation [43]:

$$P_{AC} = \frac{V_1\,V_2}{X_{12}}\sin(\delta_1 - \delta_2) \tag{10}$$

where $V_1$ and $V_2$ are the voltage magnitudes, $X_{12}$ is the line reactance, and $\delta_1$ and $\delta_2$ are the voltage angles. For small angle differences, sin $(\delta_1 - \delta_2) \approx (\delta_1 - \delta_2)$; thus, the transferred power becomes approximately dependent on the angle difference with a synchronizing coefficient $K$:

$$K = \frac{V_1\,V_2}{X_{12}} \tag{11}$$

Based on this principle, and according to AC line emulation for VSC-HVDC systems reported in [44], ADC modulates the ETL active power proportionally to the measured electrical angle difference between its terminals:

$$\Delta P_{ADC} = K_\delta\ (\delta_1 - \delta_2) \tag{12}$$

where $K_\delta$ is the control gain of the ADC. In the dynamic model, the electrical angle $\delta$ is obtained by integrating the terminal angular frequency $\omega$ (where $\omega = 2\pi f$). Accordingly, the angle difference is given by [45,46]

$$\Delta\delta = \delta_1 - \delta_2 = \int (\omega_1 - \omega_2)\, dt \tag{13}$$

By implementing this concept, the VSC-HVDC link injects synchronizing power in a similar way to an AC line does, which enhances transient stability after disturbances.

- Frequency-Difference Control (FDC)

FDC introduces active power modulation proportionally to the frequency difference between the two VSC-HVDC terminals. This controller provides damping power, which helps to increase the transient stability margin and damp power oscillations [47]:

$$\Delta P_{FDC} = K_{\omega}\ (f_1 - f_2) \tag{14}$$

where $K_{\omega}$ is the control gain of FDC, and $f_1$ and $f_2$ are the measured frequencies at the HVDC terminals.

- Feedforward Action

The feedforward action provides a fast response for VSC-HVDC by comparing the scheduled power with the instantaneous measured power. This action helps reallocate power and compensate for known or predictable disturbances, enabling fast redistribution of power and supporting primary and secondary frequency control. The feedforward control law is [48]

$$\Delta P_{FF} = K_{ff}\ (P_0 - P_{meas}) \tag{15}$$

where $K_{ff}$ is the control gain of feedforward, $P_0$ is the scheduled power setpoint, and $P_{meas}$ is the measured VSC-HVDC power flow. The overall proposed supplementary control scheme is illustrated in Figure 5.

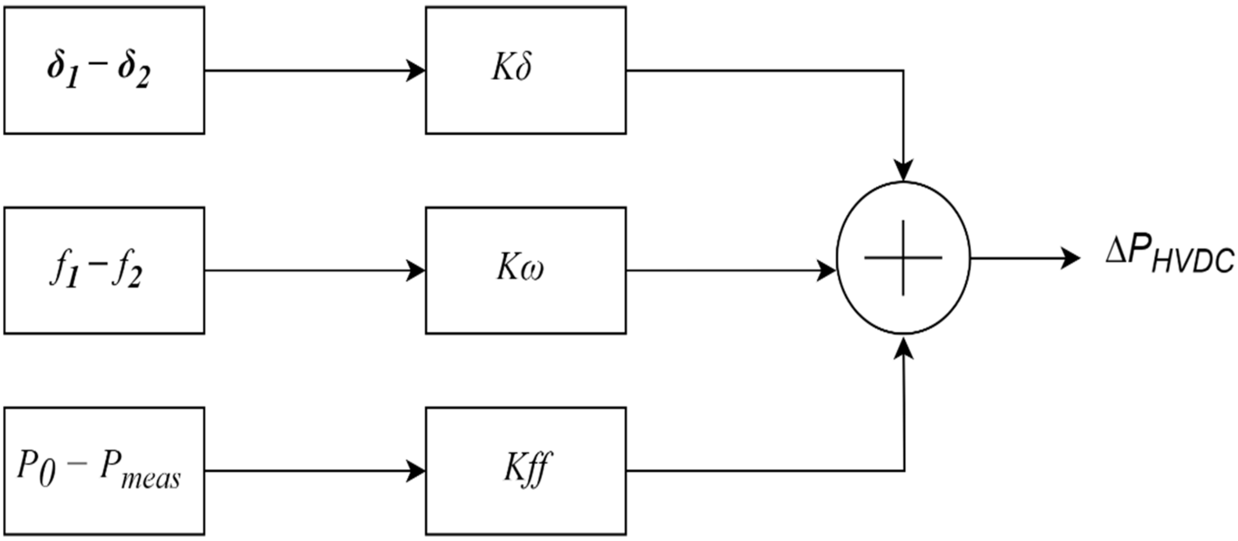


**Figure 5.** Schematic diagram of the proposed supplementary control strategy for the ETL.

## 5. Applications and Studies

By implementing the proposed control layer within the dynamic model of the VSC-HVDC link, the contribution of the ETL to post-splitting frequency stability is assessed under severe contingency conditions.

*Static Operating Point Analysis*

The operating point considered in this study corresponds to the 2030 forecast scenario, based on detailed grid studies and planning models developed by the Italian research center RSE (Ricerca sul Sistema Energetico). The analyzed condition is the system splitting following the loss of the Sicily–Calabria AC interconnection, which results in an 800 MW over-generation in Sicily. At this operating point, the Sicilian power system exhibits low primary frequency regulation reserves due to high RES generation. Figure 6 illustrates the interconnections between Sicily and the other areas in the considered operating condition with the scheduled power flow.

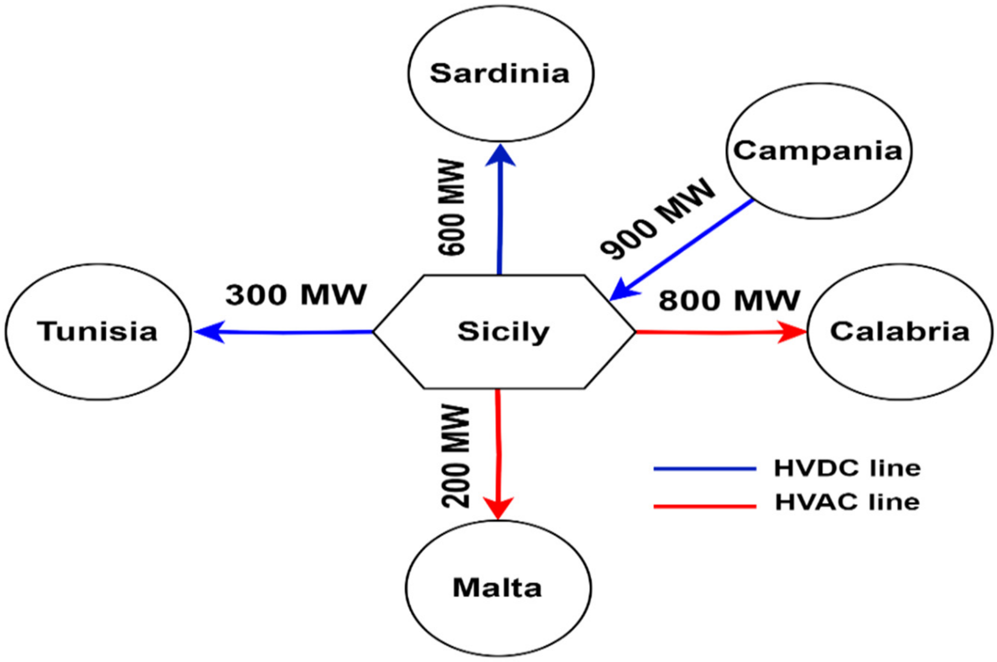


**Figure 6.** Scheme of interconnections of Sicily with interlinked regions/areas and their scheduled power flows.

Table 1 shows the technical data used for the analysis of the considered operating conditions for Sicily and Sardinia [34,43,49–52]. The simulation data are derived from 2030 forecast models developed by RSE [53], while the supplementary control gains are adopted from [41].

**Table 1.** Data for the analysis.

| Parameter | Sicily | Sardinia |
|---|---|---|
| Installed power of thermal power plants participating in frequency regulation (MW) | 2307 | 1180 |
| Power–frequency characteristics (MW/Hz) | 922.8 | 472 |
| Load (MW) | 2000 | 980 |
| RES generation (MW) | 1700 | 4143 |
| Nominal frequency (Hz) | 50 | 50 |
| Droop constant R (p.u.) | 0.05 | 0.05 |
| System inertia Hsys (s) | 2.71 | 2.71 |
| Load-regulating factor D | 0.01 | 0.01 |
| Governor time constant $T_g$ (s) | 0.5 | 0.5 |
| Turbine time constant $T_t$ (s) | 0.4 | 0.4 |
| HVDC frequency droop ($K_{f\_DC}$) (p.u.) | 50 | |
| $K_\delta$ | 17.9 | |
| $K_\omega$ | 102 | |
| $K_{ff}$ | 1 | |

Table 2 lists the thermal power plants in service during the considered contingency.

**Table 2.** Thermal power plant data.

| Sicily | Sardinia |
|---|---|
| 2 × 380 MVA CCGT<br>1 × 335 MVA CCGT<br>1 × 760 MVA CCGT<br>1 × 452 MVA CHP | 3 × 100 MVA OCGT<br>1 × 250 MVA CCGT<br>1 × 80 MVA CHP<br>1 × 550 MVA IGCC |
| CCGT: Combined Cycle Gas Turbine<br>CHP: Combined Heat and Power<br>IGCC: Integrated Gasification Combined Cycle<br>OCGT: Open Cycle Gas Turbine | |

## 6. Results and Analysis

The dynamic performance of the proposed supplementary control layer applied to the ETL is assessed under four operating conditions after a system-splitting event. The analysis focuses on frequency containment, damping characteristics, and active-power reallocation among WTL, ETL, thermal units, and RES. A comparative summary for all indicators is provided in Table 3, highlighting the incremental benefits introduced by ADC, FDC, and feedforward action.

**Table 3.** Performance metrics summary.

| Performance Metric | Condition 1 (WTL Droop Baseline) | Condition 2 (ETL − ADC) | Condition 3 (ETL − ADC + FDC) | Condition 4 (ETL − ADC + FDC + FFA) |
|---|---|---|---|---|
| **Frequency Containment (0–60 s)** | | | | |
| Sicily Frequency Zenith (Hz) | 51.05 | 50.48 | 50.45 | 50.24 |
| Sardinia Frequency Zenith (Hz) | 50.87 | 50.40 | 50.38 | 50.21 |
| Sicily Maximum RoCoF (Hz/s) | 0.20 | 0.20 | 0.19 | 0.11 |
| Sicily Steady-State Frequency (Hz) | 51.05 | 50 | 50 | 50 |
| Sardinia Steady-State Frequency (Hz) | 50.87 | 50 | 50 | 50 |
| Number of Frequency Oscillations | N/A | 8 | 7 | 0 |
| Frequency Oscillation Amplitude (Hz) | N/A | 0.03 | 0.01 | 0 |
| **Thermal Generation Response** | | | | |
| Max. Thermal Regulation (MW) | 250 | 250 | 250 | 227 |
| Residual Thermal Margin (at steady state) (MW) | 0 | 250 | 250 | 250 |
| **VSC-HVDC Active-Power Modulation** | | | | |
| Max. ETL Power Modulation (MW) | N/A | 800 | 800 | 800 |
| Max. WTL Power Modulation (MW) | 175 | 77 | 72 | 40 |
| WTL Steady-State Modulation (MW) | 175 | ≈0 | ≈0 | 0 |
| **RES (FFR + SI) Contribution** | | | | |
| SI Peak Absorption (MW) | 750 | 750 | 750 | 695 |
| RES Steady-State Contribution (MW) | 375 | 0 | 0 | 0 |

**Condition 1—WTL Droop-Based Regulation with Thermal and RES Regulation (FFR + SI)**

In this reference condition, the WTL operates under frequency-droop control and is integrated with conventional thermal units and RES to support frequency stability without ETL participation. The RES regulation combines FFR and SI, enabling fast active power support during the initial transient. The main results are summarized as follows:

- Thermal unit response: The thermal units in Sicily reduce their active power generation by approximately 250 MW, reaching their maximum regulation limits. Consequently, no further regulation can be provided, and secondary frequency control cannot be effectively activated due to the lack of remaining regulation margin.
- WTL contribution: The WTL modulates its active power according to its droop characteristic, increasing the active power transfer from Sicily to Sardinia by approximately 175 MW in addition to its scheduled power.
- RES regulation response: RES units equipped with SI absorb approximately 750 MW during the first few seconds following the disturbance, effectively limiting the frequency overshoot. RES contribution returns gradually to the droop-based regulation level of around 375 MW.
- The system remains dynamically stable; however, the steady-state frequency deviates from its nominal value. The post-fault frequency settles at 51.05 Hz in Sicily and 50.87 Hz in Sardinia, both of which remain below 51.5 Hz. Although stability is preserved, the frequency is not fully restored to the nominal value, indicating the need for additional control actions. The results are illustrated in Figures 7 and 8.

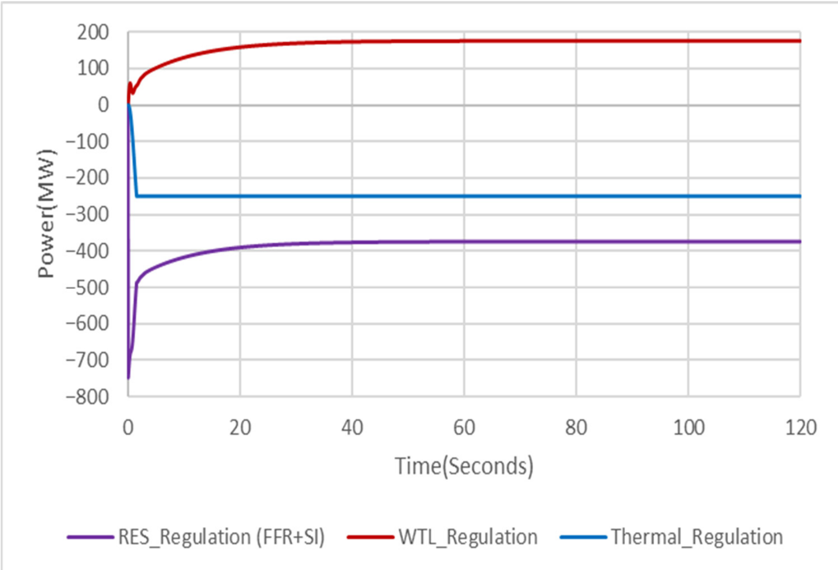


**Figure 7.** Active power response of regulating sources in Sicily, condition 1.

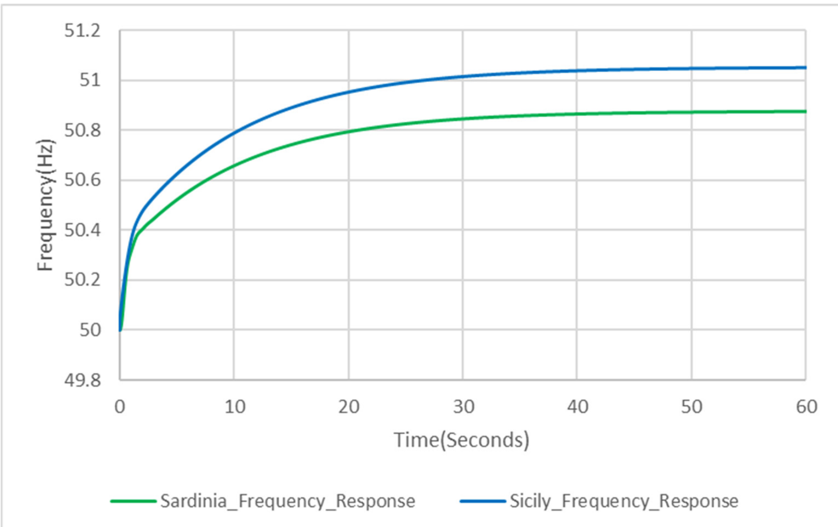


**Figure 8.** Sicily and Sardinia frequency responses, condition 1.

**Condition 2—ETL with Angle-Difference Control (ADC)**

In this condition, the ETL operates under ADC, allowing the embedded VSC-HVDC link to emulate the synchronizing behavior of an AC transmission line. Unlike condition 1, where only frequency support was provided by the WTL, thermal units, and RES. The ETL modulates its active power based on the electrical-angle separation between Sicily and the mainland of Italy. The key observations are as follows:

- Thermal unit response: The primary frequency control units in Sicily reduced their thermal generation by approximately 250 MW, reaching their maximum regulation limits. As the ETL modulates its power according to the angle difference between the two areas, the thermal output gradually returns to its scheduled value.
- ETL contribution: Immediately after the disturbance, the ETL modulates the imported active power from the mainland of Italy to Sicily according to the large electrical-angle difference resulting from the loss of the Sicily–Calabria interconnection. Through ADC, the ETL provides synchronizing power by modulating its active power in a direction that counteracts the angle deviation. In this scenario, the imported power through the ETL is reduced by approximately 800 MW, reducing the active power flow from the mainland of Italy to Sicily to 100 MW.
- WTL contribution: The WTL, operating under frequency-droop control, provides relatively small power modulation of approximately 77 MW, which is lower than in condition 1. As the ETL reduces the angle separation, the WTL gradually returns to its scheduled power.
- RES regulation response: SI absorbs approximately 750 MW during the first few seconds following the disturbance, effectively limiting the frequency overshoot and RoCoF. Once the ETL reduces the angle difference, the RES output gradually returns to its scheduled value.
- With ADC, Sicily and Sardinia experience significantly lower frequency zenith values compared with condition 1, with a zenith frequency around 50.48 Hz in Sicily and around 50.4 Hz in Sardinia. After the transient, both areas experience low-amplitude oscillations in frequency around their scheduled values, consistent with the synchronizing-power action provided by ADC. The results are illustrated in Figures 9–11.

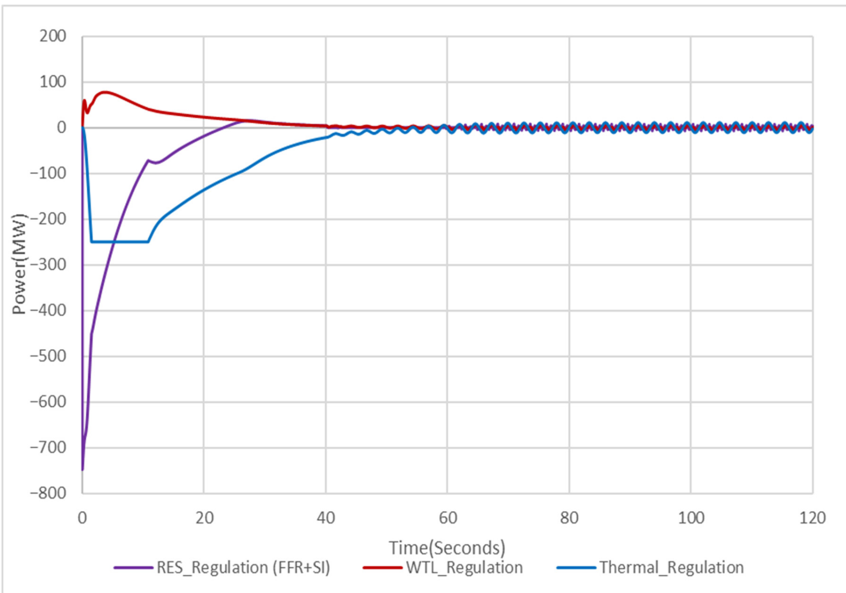


**Figure 9.** Active power response of regulating sources in Sicily, condition 2.

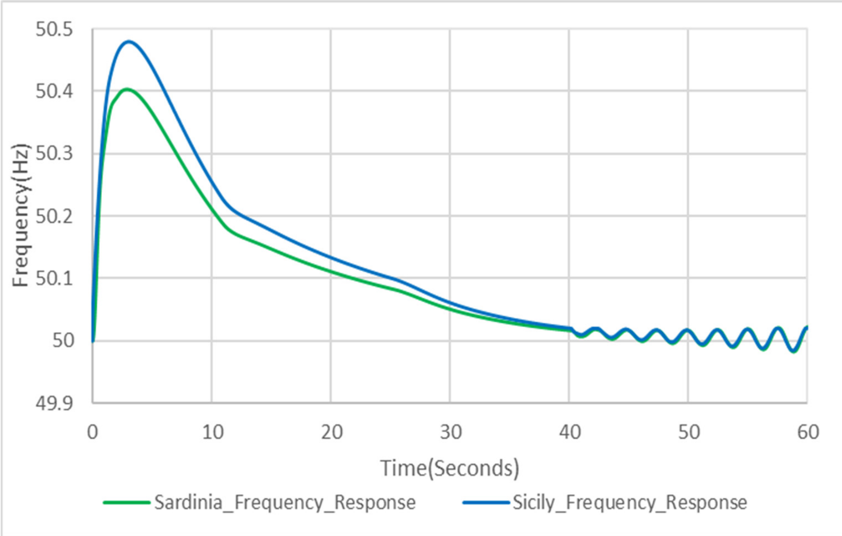


**Figure 10.** Sicily and Sardinia frequency responses, condition 2.

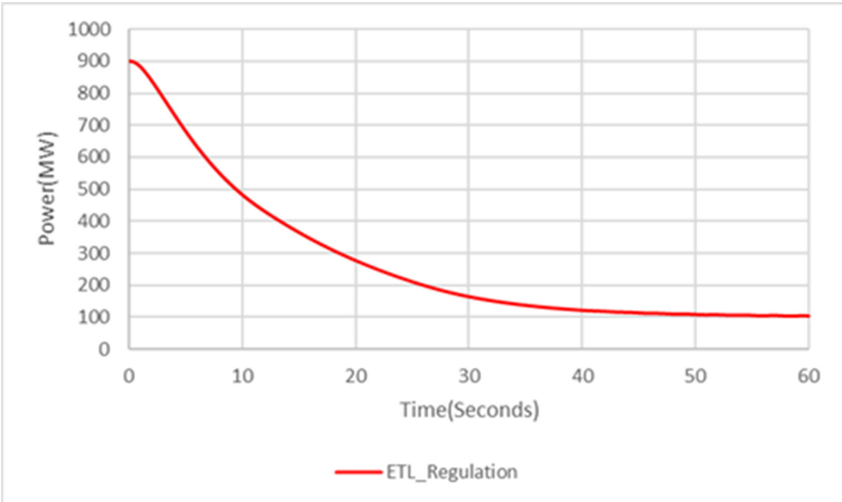


**Figure 11.** Active-power modulation of the ETL, condition 2.

**Condition 3—ETL with Combined ADC + FDC**

In this condition, the ETL operates with a combined supplementary control scheme that includes both ADC and FDC, where ADC restores the angle difference resulting from system splitting, while FDC introduces damping power proportional to the frequency difference between Sicily and the mainland of Italy. This coordination enhances the dynamic performance compared with condition 2, as follows:

- Thermal unit response: Thermal units provide primary regulation by reducing their active power output, similarly to condition 2, reaching their maximum regulation limits. However, due to the additional damping power introduced by FDC, thermal output gradually and smoothly returns to its normal operating point, with lower oscillations.
- ETL contribution: The ETL provides the same synchronizing power as in condition 2 through ADC. With the addition of FDC, ETL provides damping power and helps to eliminate the oscillations in all system variables (frequency and power flows).
- WTL contribution: The WTL modulates its active power according to its droop characteristic, with a peak modulation of approximately 72 MW and lower oscillations due to the damping power introduced by the ETL, resulting in stable operation and low mechanical stress on the link.

- RES regulation response: SI absorbs approximately 750 MW during the first few seconds following the disturbance, similarly to condition 2; RES units experience a smooth transient, with lower oscillations due to the damping power introduced by FDC.
- The implementation of ADC and FDC results in a clear improvement, since the zenith frequency in Sicily is slightly reduced to approximately 50.45 Hz and 50.38 Hz in Sardinia, with low oscillations appearing during the dynamic frequency response. The results are illustrated in Figures 12–14.

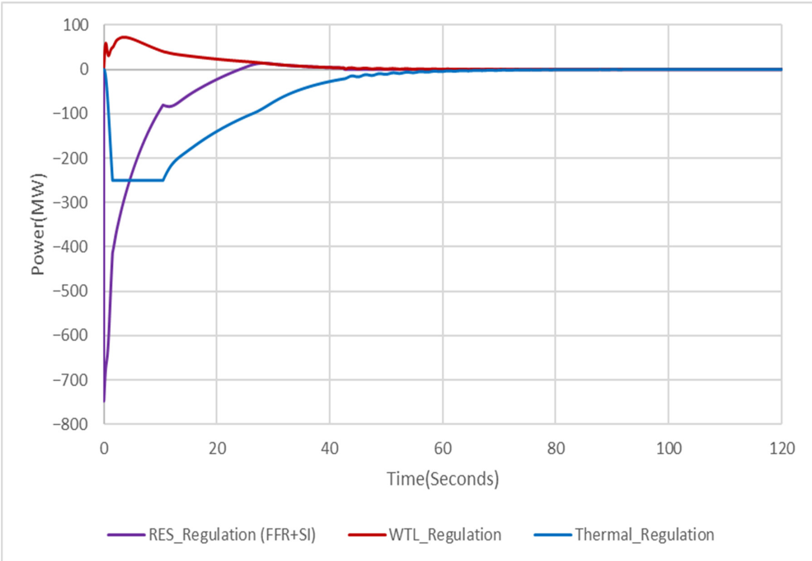


**Figure 12.** Active power response of regulating sources in Sicily, condition 3.

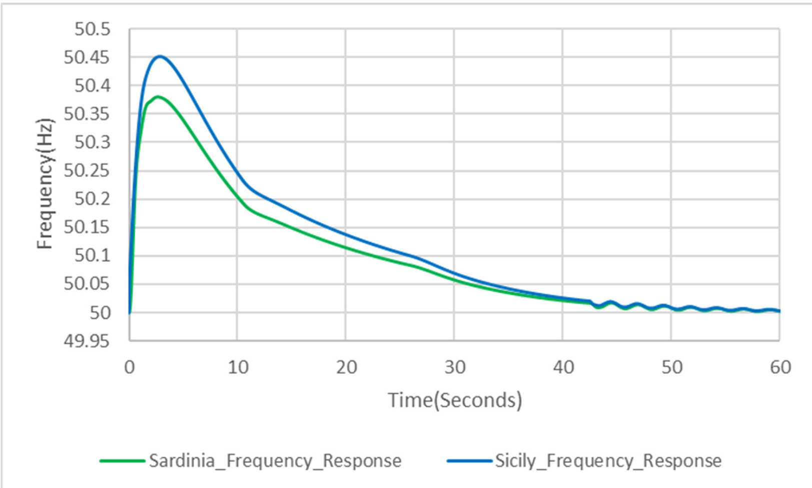


**Figure 13.** Sicily and Sardinia frequency responses, condition 3.

**Condition 4—ETL with Full Supplementary Control (ADC + FDC + Feedforward)**

In this condition, the ETL operates under the complete supplementary control layer, while ADC restores synchronization, and FDC provides damping power. The feedforward enables rapid reallocation of power transfer between Sicily and mainland Italy following the disturbance by comparing the scheduled value with the measured value:

- Thermal unit response: Thermal units reduce their active power output by around 227 MW due to the rapid compensation provided by the ETL. Thermal regulation did not reach its maximum limits, which provides valuable regulation margin for secondary frequency control, an important requirement in low-inertia systems, and it smoothly returns to its normal operating point.

- ETL contribution: The ETL provides the most effective response in this condition, since ADC restores the pre-fault angle by providing synchronizing power, reducing the power import from mainland Italy. FDC injects damping power, reducing the frequency oscillation observed in condition 2. Feedforward action provides fast power compensation for the power imbalance, which accelerates the redistribution of the power between Sicily and the mainland of Italy.
- WTL contribution: The WTL provides a small active power modulation of approximately 40 MW, which is the lowest among all conditions with low oscillations, resulting in reduced mechanical and electrical stress on the link.
- RES regulation response: RES units equipped with SI absorb around 750 MW in the first few seconds, limiting the RoCoF and the frequency overshoot. The presence of feedforward allows the RES output to return quickly to its scheduled value.
- The combined supplementary control of ADC, FDC, and feedforward results in the optimal dynamic frequency performance among all conditions. The zenith frequency for Sicily is reduced to 50.24 Hz. In Sardinia, the zenith frequency is also reduced to 50.21 Hz due to the lowest active power modulation by the WTL. The system frequency returns close to nominal without experiencing sustained oscillations. The results are illustrated in Figures 5–17.

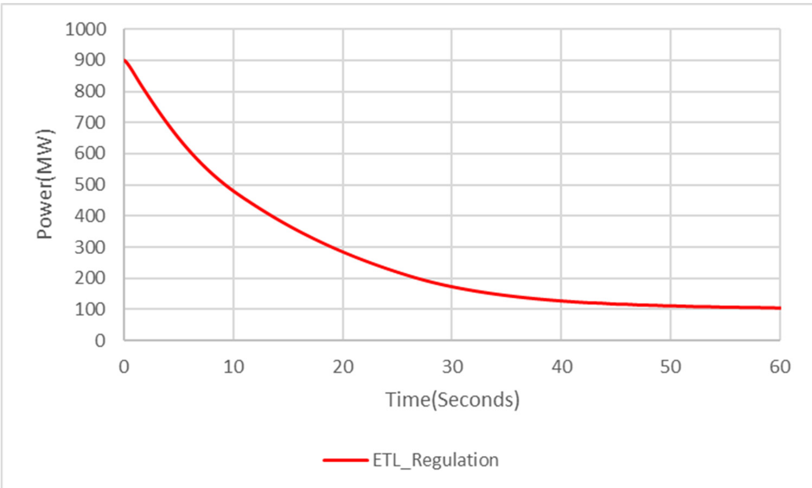


**Figure 14.** Active-power modulation of the ETL, condition 3.

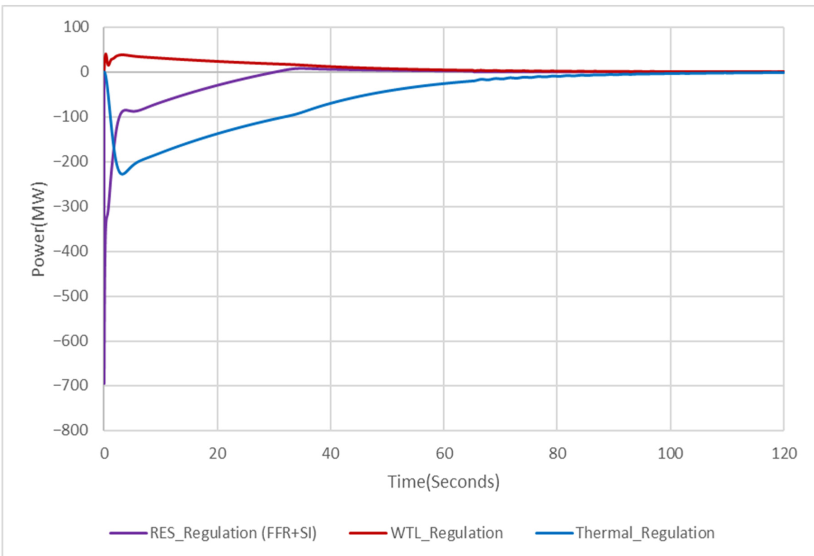


**Figure 15.** Active power response of regulating sources in Sicily, condition 4.

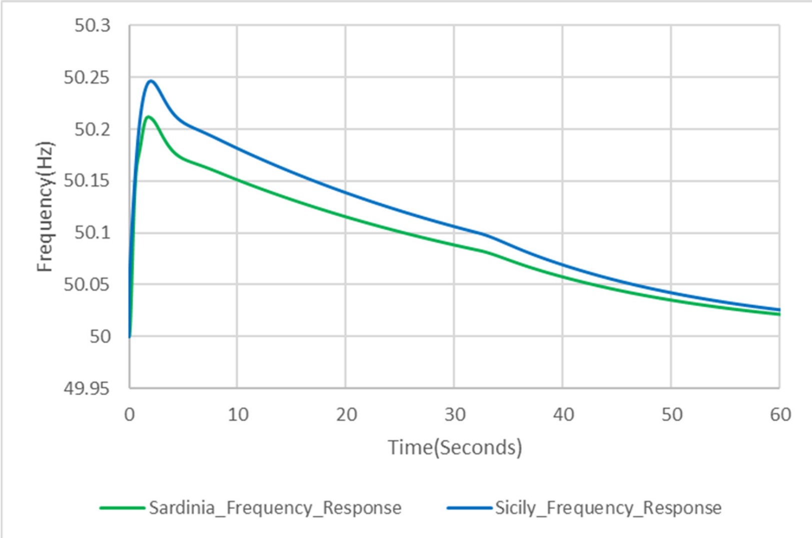


**Figure 16.** Sicily and Sardinia frequency responses, condition 4.

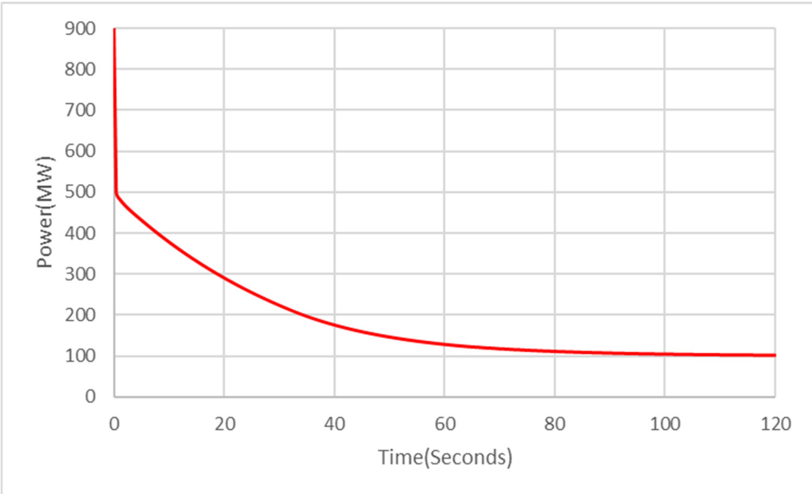


**Figure 17.** Active-power modulation of the ETL, condition 4.

Table 3 summarizes the main performance metrics for the four conditions, clearly highlighting the progressive improvement in frequency containment, damping characteristics, and active-power reallocation as additional supplementary control actions are introduced.

## 7. Conclusions

This paper investigates the capability of an embedded VSC-HVDC interconnection to support frequency stability following system-splitting events by proposing and evaluating a coordinated supplementary control layer integrated within a dynamic LFC model. The analysis focuses on the ETL, considering a severe over-generation scenario resulting from the loss of synchronism between Sicily and the mainland of Italy in a 2030 scenario.

The proposed control strategy combines ADC, FDC, and feedforward action to enable the ETL to actively participate in post-splitting frequency stability. Simulation results demonstrate that, under the reference condition, relying solely on thermal unit regulation, RES regulation, and WTL droop control is insufficient to restore the system frequency to its nominal value. Moreover, the thermal units reach their maximum regulation capability, while RES and WTL provide high levels of power regulation, which reduces system stiffness to address additional disturbances.

The introduction of ADC enables the ETL to emulate the synchronizing behavior of an AC transmission line, reducing the frequency zenith, improving the transient response, and restoring the system frequency close to its nominal value. In addition, ADC reduces the regulation burden on both RES and the WTL. However, the implementation of ADC alone results in low-frequency oscillations due to the absence of damping power.

FDC plays an important role in mitigating these oscillations by providing the required damping power, resulting in a smooth and stable response. The implementation of ADC and FDC preserves the frequency improvement achieved by ADC while eliminating the observed oscillations. By implementing the complete supplementary control layer, combining ADC, FDC, and feedforward action, the optimal dynamic performance among all cases is achieved. In this case, the frequency zenith is significantly reduced, system resilience is enhanced, the thermal units do not reach their maximum regulation limits, and limited WTL modulation is required, ensuring that the additional power export to Sardinia does not threaten its frequency stability.

Overall, the results highlight the important role that embedded VSC-HVDC systems can play in supporting frequency stability in future low-inertia power systems under post-splitting conditions when equipped with advanced control strategies. Although embedded VSC-HVDC links operate within the same synchronous area under normal operating conditions, they can provide fast, robust frequency support following system separation. Moreover, by restoring both electrical angle and frequency at their terminals, the proposed control scheme facilitates favorable conditions for secure system reconnection and prevents undesired power flow through AC interconnections. The detailed synchronization and reconnection process will be addressed in future work. These results confirm that appropriately controlled embedded VSC-HVDC links are essential for enhancing resilience and operational flexibility in future power systems with high-RES penetration.

**Author Contributions:** Conceptualization, A.L., M.Q. and G.Z.; methodology, A.V., M.Q. and G.Z.; software, M.Q. and A.V.; validation, A.L., L.C.V. and G.Z.; formal analysis, L.M. and A.V.; resources, A.L. and L.C.V.; data curation, A.L. and L.C.V.; writing—original draft preparation, M.Q., L.M. and A.V.; supervision, G.Z.; project administration, A.L.; funding acquisition, G.Z. All authors have read and agreed to the published version of the manuscript.

**Funding:** This work has been partly financed by the Research Fund for the Italian Electrical System under the Three-Year Research Plan 2025–2027 (MASE Decree n. 388 of 6th November 2024), in compliance with the MASE Decree n. 139 of 12 April 2024, and by the EU funds of Next-Generation EU (Piano Nazionale di Ripresa e Resilienza, PNRR—Missione 4, Componente 2, Linea di Investimento 3.3—MUR Decree n. 630 of 24 April 2024).

**Data Availability Statement:** Data used in this study can be found in the papers from the same research group cited in the manuscript.

**Conflicts of Interest:** The authors declare no conflicts of interest.

## Abbreviations

The following abbreviations are used in this manuscript:

| | |
|---|---|
| AC | Alternating Current |
| ADC | Angle-Difference Control |
| CESA | Continental Europe Synchronous Area |
| DC | Direct Current |
| ENTSO-E | European Network of Transmission System Operators for Electricity |
| ETL | East Tyrrhenian Link |
| FFR | Fast Frequency Response |
| FDC | Frequency-Difference Control |

| | |
|---|---|
| HVAC | High-Voltage Alternating Current |
| HVDC | High-Voltage Direct Current |
| LFC | Load Frequency Control |
| RES | Renewable Energy Sources |
| RoCoF | Rate of Change in Frequency |
| SI | Synthetic Inertia |
| TL | Tyrrhenian Link |
| VSC | Voltage Source Converter |
| WTL | West Tyrrhenian Link |

## References


1. European Commission. *Communication from the Commission to the European Parliament, the European Council, the Council, the European Economic and Social Committee and the Committee of the Regions*; COM(2019) 640 Final, The European Green Deal; European Commission: Brussels, Belgium, 2019.
2. European Commission. *Communication from the Commission to the European Parliament, the Council, the European Economic and Social Committee and the Committee of the Regions 'Fit for 55': Delivering the EU's 2030 Climate Target on the Way to Climate Neutrality*; COM/2021/550 Final of 14.7.2021; European Commission: Brussels, Belgium, 2021.
3. European Commission. *Communication from the Commission to the European Parliament, the European Council, the Council, the European Economic and Social Committee and the Committee of the Regions REPowerEU Plan*; COM(2022) 230 Final of 18.05.2022; European Commission: Brussels, Belgium, 2022.
4. Di Gloria, P.; Paradiso, S.; Pede, M.; Sorrentino, V.M.E.; Vergine, C.; Massaro, F.; Vasile, A.; Zizzo, G. On the Impact of Renewable Generation on the Sicilian Power System in Near-Future Scenarios: A Case Study. *Energies* **2024**, *17*, 3352. [CrossRef]
5. Watson, N.R.; Watson, J.D. An Overview of HVDC Technology. *Energies* **2020**, *13*, 4342. [CrossRef]
6. Bin, Z.; Feng, X.; Miao, Z.; Kong, X.; Li, P.; Shao, B. Frequency Characteristic Analysis of the VSC-HVDC DC Oscillating Power under AC Sub-Synchronous Disturbances. *Electronics* **2024**, *13*, 3445. [CrossRef]
7. Henry, S.; Despouys, O.; Adapa, R.; Barthold, C.; Bell, K.; Binard, J.L.; Edris, A.; Egrot, P.; Hung, W.; Irwin, G.; et al. *Influence of Embedded HVDC Transmission on System Security and AC Network Performance*; Conseil International des Grands Réseaux Électriques, Ed.; CIGRÉ: Paris, France, 2013; ISBN 978-2-85873-230-2.
8. Yu, J.; Karady, G.; Qin, J. Controls of Embedded HVDC System for System Dynamic Performance Enhancement. In *Proceedings of the 2017 IEEE Power & Energy Society General Meeting*; IEEE: Chicago, IL, USA, 2017; pp. 1–5.
9. Terna: 2023 Development Plan for the National Electricity Grid Presented—Terna Spa. Available online: https://www.terna.it/en/media/press-releases/detail/2023-development-plan (accessed on 26 March 2026).
10. Wang, K.; Zhou, C.; Chen, Y.; Guo, Y.; Fan, Z.; Li, Z. Investigation of Frequency Response Sharing-Induced Power Oscillations in VSC-HVDC Systems for Asynchronous Interconnection. *Energies* **2025**, *18*, 2928. [CrossRef]
11. ENTSO-E. *Embedded HVDC Systems—Frequency Schemes in Case of System Split: ENTSO-E Guidance Document for National Implementation for Network Codes on Grid Connection*; ENTSO-E: Brussels, Belgium, 2018.
12. Qawaqneh, M.; Zizzo, G.; Vasile, A.; Favuzza, S.; L'Abbate, A.; Vitulano, L. Evaluating Renewable Energy Control Strategies Integrated with HVDC Droop Control for Sicily's Frequency Stability. In Proceedings of the 2025 AEIT HVDC International Conference (AEIT HVDC), Genova, Italy, 29–30 May 2025; pp. 1–5.
13. Qawaqneh, M.; Zizzo, G.; Vasile, A.; Favuzza, S.; L'Abbate, A.; Vitulano, L. Assessment of Secondary Frequency Control and Synthetic Inertia Contribution of RES to Sicily's Frequency Stability. In Proceedings of the 2025 AEIT International Annual Conference (AEIT), Fukuoka, Japan, 10–12 September 2025; pp. 1–6.
14. Ciapessoni, E.; Cirio, D.; Gatti, A.; Pitto, A. Renewable Power Integration in Sicily: Frequency Stability Issues and Possible Countermeasures. In Proceedings of the 2013 IREP Symposium Bulk Power System Dynamics and Control—IX Optimization, Security and Control of the Emerging Power Grid, Crete, Greece, 25–30 August 2013; pp. 1–7.
15. Adu, J.A.; Tossani, F.; Pontecorvo, T.; Ilea, V.; Vicario, A.; Conte, F.; D'Agostino, F. Coordinated Inertial Response Provision by Wind Turbine Generators: Effect on Power System Small-Signal Stability of the Sicilian Network. In Proceedings of the 2022 IEEE International Conference on Environment and Electrical Engineering and 2022 IEEE Industrial and Commercial Power Systems Europe (EEEIC/I&CPS Europe), Prague, Czech Republic, 28 June–1 July 2022; pp. 1–6.
16. Berizzi, A.; Ilea, V.; Vicario, A.; Conte, F.; Massucco, S.; Adu, J.A.; Nucci, C.A.; Pontecorvo, T. Stability Analysis of the OSMOSE Scenarios: Main Findings, Problems, and Solutions Adopted. In Proceedings of the 2021 AEIT International Annual Conference (AEIT), Milan, Italy, 4–8 October 2021; pp. 1–6.
17. Adu, J.A.; Berizzi, A.; Conte, F.; D'Agostino, F.; Ilea, V.; Napolitano, F.; Pontecorvo, T.; Vicario, A. Power System Stability Analysis of the Sicilian Network in the 2050 OSMOSE Project Scenario. *Energies* **2022**, *15*, 3517. [CrossRef]

18. Giannuzzi, G.M.; Palone, F.; Rebolini, M.; Vassallo, J.; Zaottini, R. The Malta-Sicily EHV-AC Interconnector. In Proceedings of the 8th Mediterranean Conference on Power Generation, Transmission, Distribution and Energy Conversion (MEDPOWER 2012), Cagliari, Italy, 1–3 October 2012; p. 87. [CrossRef]
19. Del Pizzo, F.; Carlini, E.M.; Scirocco, T.B.; Dicuonzo, F.; Urbanelli, A.; Zanghì, A.; Armillei, C. Tyrrhenian Link: Path towards a Decarbonized Electrical System. In Proceedings of the 2022 AEIT International Annual Conference (AEIT), Rome, Italy, 3–5 October 2022; pp. 1–6.
20. Musca, R.; Sanseverino, E.R.; Zizzo, G.; L'Abbate, A. An Accurate Model for Steady-State and Dynamic Analysis of the Sicilian Network with HVDC Interconnections. In Proceedings of the 17th International Conference on AC and DC Power Transmission (ACDC 2021), Virtual, Online, 7–8 December 2021; Volume 2021, pp. 188–192.
21. Derviskadic, A.; Persico, A.; Isabegovic, E.; Thorslund, A. Opportunities and Challenges in the Mediterranean Region with Grid Forming Control for HVDC Systems. In Proceedings of the 2023 AEIT HVDC International Conference (AEIT HVDC), Rome, Italy, 25–26 May 2023; pp. 1–6.
22. ENTSO-E SPD (System Protection & Dynamics) Subgroup. *Frequency Stability Evaluation Criteria for the Synchronous Zone of Continental Europe—Requirements and Impacting Factors*; ENTSO-E: Brussels, Belgium, 2016.
23. Conte, F.; Crosa di Vergagni, M.; Massucco, S.; Silvestro, F.; Ciapessoni, E.; Cirio, D. Performance Analysis of Frequency Regulation Services Provided by Aggregates of Domestic Thermostatically Controlled Loads. *Int. J. Electr. Power Energy Syst.* **2021**, *131*, 107050. [CrossRef]
24. Conte, F.; Massucco, S.; Silvestro, F.; Ciapessoni, E.; Cirio, D. Stochastic Modelling of Aggregated Thermal Loads for Impact Analysis of Demand Side Frequency Regulation in the Case of Sardinia in 2020. *Int. J. Electr. Power Energy Syst.* **2017**, *93*, 291–307. [CrossRef]
25. Al Kez, D.; Foley, A.M.; Ahmed, F.W.; O'Malley, M.; Muyeen, S.M. Potential of Data Centers for Fast Frequency Response Services in Synchronously Isolated Power Systems. *Renew. Sustain. Energy Rev.* **2021**, *151*, 111547. [CrossRef]
26. Akram, U.; Nadarajah, M.; Shah, R.; Milano, F. A Review on Rapid Responsive Energy Storage Technologies for Frequency Regulation in Modern Power Systems. *Renew. Sustain. Energy Rev.* **2020**, *120*, 109626. [CrossRef]
27. Li, S.; Xu, Q.; Xia, Y.; Hua, K. Comprehensive setting and optimization of Dead-Band for BESS participate in power grid primary frequency regulation. *Int. J. Electr. Power Energy Syst.* **2022**, *151*, 107050. [CrossRef]
28. Huang, H.; Li, F. Sensitivity Analysis of Load-Damping Characteristic in Power System Frequency Regulation. *IEEE Trans. Power Syst.* **2013**, *28*, 1324–1335. [CrossRef]
29. Favuzza, S.; Ippolito, M.G.; Massaro, F.; Paternò, G.; Puccio, A. 2015–2020. Sicily and Italy as Electricity Hub in the Mediterranean Area for the Development of the European Power Grids Interconnections. In Proceedings of the 2015 IEEE 5th International Conference on Power Engineering, Energy and Electrical Drives (POWERENG), Riga, Latvia, 11–13 May 2015; pp. 554–559.
30. ENTSO-E. *Operation Handbook OpHB, Policy 1: Load-Frequency Control and Performance*, Version 3.0; ENTSO-E: Brussels, Belgium, 2009.
31. ENTSO-E. *Report on Deterministic Frequency Deviations: Root Causes and Proposals for Potential Solutions*; ENTSO-E: Brussels, Belgium, 2020.
32. Pandey, S.K.; Jahan, N. Load Frequency Control of Single Area Power System Using LQG Controller. In Proceedings of the 2022 2nd International Conference on Innovative Practices in Technology and Management (ICIPTM), Pradesh, India, 23–25 February 2022; Volume 2, pp. 503–507.
33. Fang, C.; Tang, Y.; Ye, R.; Lin, Z.; Zhu, Z.; Wen, B.; Ye, C. Adaptive Control Strategy of Energy Storage System Participating in Primary Frequency Regulation. *Processes* **2020**, *8*, 687. [CrossRef]
34. Massaro, F.; Musca, R.; Vasile, A.; Zizzo, G. A Simulation Study for Assessing the Impact of Energy Storage Systems for Fast Reserve with Additional Synthetic Inertia Control on the Continental Europe Synchronous Area. *Sustain. Energy Technol. Assess.* **2022**, *53*, 102763. [CrossRef]
35. Jietan, Z.; Linan, Q.; Pestana, R.; Fengkui, L.; Libin, Y. Dynamic Frequency Support by Photovoltaic Generation with "Synthetic" Inertia and Frequency Droop Control. In Proceedings of the 2017 IEEE Conference on Energy Internet and Energy System Integration (EI2), Beijing, China, 26–28 November 2017; pp. 1–6.
36. Bruno, S.; Giannoccaro, G.; Iurlaro, C.; La Scala, M.; Rodio, C. Power Hardware-in-the-Loop Test of a Low-Cost Synthetic Inertia Controller for Battery Energy Storage System. *Energies* **2022**, *15*, 3016. [CrossRef]
37. Jiang, H.; Zhou, Y.; Gao, Y.; Gao, S. Droop Frequency Limit Control and Its Parameter Optimization in VSC-HVDC Interconnected Power Grids. *Energies* **2024**, *17*, 3851. [CrossRef]
38. Vinoth Kumar, N.J.; Thameem Ansari, M.M. A New Design of Dual Mode Type-II Fuzzy Logic Load Frequency Controller for Interconnected Power Systems with Parallel AC–DC Tie-Lines and Capacitor Energy Storage Unit. *Int. J. Electr. Power Energy Syst.* **2016**, *82*, 579–598. [CrossRef]


https://doi.org/10.3390/en19092034

39. Torres, J.L.R.; Perilla, A.; Rakhshani, E.; Palensky, P.; van der Meijden, M.A.A.M.; Alefragkis, A. MVMO-Based Tuning of Active Power Gradient Control of VSC-HVDC Links for Frequency Support. In Proceedings of the 2019 2nd International Conference on Smart Grid and Renewable Energy (SGRE), Doha, Qatar, 19–21 November 2019; pp. 1–6.
40. Shen, L.; Barnes, M.; Preece, R.; Milanović, J. Frequency Stabilisation Using VSC-HVDC. In Proceedings of the 2016 IEEE Power and Energy Society General Meeting (PESGM), Boston, MA, USA, 17–21 July 2016; pp. 1–5.
41. Carlos Gonzalez-Torres, J.; Costan, V.; Damm, G.; Benchaib, A.; Lamnabhi-Lagarrigue, F. Dynamic Control of Embedded HVDC to Contribute to Transient Stability Enhancement. In Proceedings of the CIGRE 2020 e-Session, Paris, France, 23–28 August 2020.
42. Song, S.; Kim, J.; Lee, J.; Jang, G. AC Transmission Emulation Control Strategies for the BTB VSC HVDC System in the Metropolitan Area of Seoul. *Energies* **2017**, *10*, 1143. [CrossRef]
43. Kundur, P.S. Power System Stability. In *Power System Stability and Control*; CRC Press: Boca Raton, FL, USA, 2012.
44. Renedo, J.; Sigrist, L.; Rouco, L.; Garcia-Cerrada, A. Impact on Power System Transient Stability of AC-Line-Emulation Controllers of VSC-HVDC Links. In Proceedings of the 2021 IEEE Madrid PowerTech, Madrid, Spain, 28 June–2 July 2021; pp. 1–6.
45. Prakash, A.; Kumar, K.; Parida, S.K. PIDF(1+FOD) Controller for Load Frequency Control with SSSC and AC–DC Tie-line in Deregulated Environment. *IET Gener. Trans. Dist.* **2020**, *14*, 2751–2762. [CrossRef]
46. Nath, V.; Sambariya, D.K. Optimal Load Frequency Control for Interconnected Power Systems Using Optimized PI-PD Controller with TCSC and HVDC Integration. *Indones. J. Electr. Eng. Inform. (IJEEI)* **2023**, *11*, 987–1006. [CrossRef]
47. Sigrist, L.; Echavarren, F.; Rouco, L.; Panciatici, P. A Fundamental Study on the Impact of HVDC Lines on Transient Stability of Power Systems. In Proceedings of the 2015 IEEE Eindhoven PowerTech, Eindhoven, The Netherlands, 29 June–2 July 2015; pp. 1–6.
48. Eriksson, R.; Knazkins, V.; Soder, L. On the Assessment of the Impact of a Conventional HVDC on a Test Power System. In Proceedings of the 2007 iREP Symposium—Bulk Power System Dynamics and Control—VII, Revitalizing Operational Reliability, Charleston, SC, USA, 19–24 August 2007; pp. 1–5.
49. Wang, Y.; Zhu, J.; Zeng, Q.; Zheng, Z.; Yu, G.; Yin, A. Frequency Coordinated Control Strategy for an HVDC Sending-End System with Wind Power Integration Based on Fuzzy Logic Control. *Energies* **2021**, *14*, 6095. [CrossRef]
50. ENTSO-E. *Inertia and Rate of Change of Frequency (RoCoF): Version 17—SPD—Inertia TF*; ENTSO-E: Brussels, Belgium, 2020.
51. Ippolito, M.G.; Musca, R.; Zizzo, G. Generalized Power-Angle Control for Grid-Forming Converters: A Structural Analysis. *Sustain. Energy Grids Netw.* **2022**, *31*, 100696. [CrossRef]
52. Mosca, C.; Bompard, E.; Aluisio, B.; Migliori, M.; Vergine, C.; Cuccia, P. HVDC for Frequency Stability under RES Penetration: The Sardinia Island Case. In Proceedings of the 2019 AEIT HVDC HVDC International Conference (AEIT HVDC), Florence, Italy, 9–10 May 2019; pp. 1–6.
53. Musca, R.; Sanseverino, E.R.; Vasile, A.; Zizzo, G.; Iaria, A.; L'Abbate, A.; Vitulano, L. Power-Flow Studies on the Future Electricity Grid of Sicily: Analysis of 2030 Scenario Cases. In Proceedings of the 2023 AEIT International Annual Conference (AEIT), Rome, Italy, 5–7 October 2023; pp. 1–6.


**Disclaimer/Publisher's Note:** The statements, opinions and data contained in all publications are solely those of the individual author(s) and contributor(s) and not of MDPI and/or the editor(s). MDPI and/or the editor(s) disclaim responsibility for any injury to people or property resulting from any ideas, methods, instructions or products referred to in the content.